Received: 12 March 2024 | Revised: 17 June 2024 | Accepted: 29 July 2024

DOI: 10.1111/jfb.15903

REGULAR ARTICLE

JOURNAL OF FISH BIOLOGY fsbi

Drivers of growth in strong year classes of the deepwater redfish (*Sebastes mentella*) population from the Gulf of St. Lawrence derived from otolith increment-based growth chronologies

Lola Coussau[1] | Olivier Morissette[2] | Dominique Robert[1] | Pascal Sirois[2]

[1]Institut des Sciences de la Mer de Rimouski, Université du Québec à Rimouski, Rimouski, Quebec, Canada

[2]Département des Sciences Fondamentales, Université du Québec à Chicoutimi, Chicoutimi, Quebec, Canada

Correspondence
Lola Coussau, Institut des Sciences de la Mer de Rimouski, Université du Québec à Rimouski, Rimouski, QC, Canada.
Email: lola.coussau@uqar.ca

Funding information
Fisheries and Oceans Canada (DFO); Ressources Aquatiques Québec (RAQ); Fonds de recherche du Québec—Nature et technologies (FRQNT), Grant/Award Number: 2020-RS4-265329; Canada Research Chair Program

Abstract

The case of the deepwater redfish (*Sebastes mentella*) in the Gulf of St. Lawrence (GSL) is a compelling example of drastic fluctuations in annual recruitment strength, characteristic of spasmodic stocks. After three decades of low abundance, the emergence of three consecutive strong year classes in 2011–2013 resulted in an unprecedented increase in biomass. In spasmodic stocks such as GSL redfish, strong year classes sustain both the biomass and catch for decades. Therefore, understanding the growth dynamics of these cohorts is essential. In the present study, we reconstructed the annual growth rates of redfish using otolith increment-based annual chronology and investigated the drivers of growth variation in redfish strong year classes of the early 2010s and early 1980s. Stock biomass was identified as the main extrinsic driver of redfish growth, suggesting intense competition for food at high conspecific density. Warming of deep waters in the GSL, where adult redfish settle, positively correlated with individual growth. However, recent warming of the cold intermediate layer showed a negative correlation with redfish growth, likely related to the shrinking of the habitat this water mass provides for various redfish cold-water prey rather than to a direct effect of temperature. Reconstruction of redfish annual growth trajectories from birth to capture emphasized the importance of carryover effects in the growth potential of strong year classes. This work provided an important first outlook of the factors driving growth variation in GSL redfish spasmodic stock and explored midterm consequences of density-dependent pressures on biological parameters of the population.

KEYWORDS
annual increment, density dependence, growth, Gulf of St. Lawrence, mixed-effects models, otolith

1 | INTRODUCTION

The causes and consequences of fluctuations in the size of marine fish populations have extensively been investigated by fish biologists to develop sustainable exploitation strategies in the context of the acceleration of global environmental changes. The main factors driving these fluctuations are environmental and demographic, either operating alone or in combination, with their effects often amplified by fishing pressure (Shelton & Mangel, 2011; van der Sleen et al., 2018). In the context of ongoing global change, temperature has received the most attention across diverse species, developmental stages, and ecosystems (Parmesan & Yohe, 2003; Poloczanska et al., 2013). Evidence shows that temperature changes have significant impacts on fish populations. First, temperature changes alter fish vital rates such as growth, maturation, sexual investment, and survival through direct effects on physiological and metabolic processes (Fry, 1971; Little et al., 2020). Additionally, temperature changes affect species abundance and distribution (Campana et al., 2020), prey community composition (Perry et al., 2005), and trophic interactions (Durant et al., 2019; Edwards & Richardson, 2004). Density-dependent survival and growth are other important mechanisms regulating the size of fish populations through a stock–recruitment relationship for prerecruits (Beverton & Holt, 1957; Pepin, 2015; Ricker, 1954) or food competition for the post-recruit (Lorenzen & Enberg, 2002).

Density-dependence effects on growth can be particularly strong in slow-growing and long-lived fish species characterized by spasmodic recruitment (Caddy & Gulland, 1983; Licandeo et al., 2020; Norse et al., 2012). In these species, the rare occurrence of strong year classes is generally linked to relatively slow growth due to compensatory density dependence (Rose et al., 2001; Saborido-Rey et al., 2004; Whitten et al., 2013) resulting from reduced feeding success under strong competition for food at high conspecific density (Andersen et al., 2017; Smith & Reay, 1991). These stocks are inherently vulnerable to sudden decline even in the absence of fishing pressure (Caddy & Gulland, 1983), so that understanding the drivers of growth is essential to develop management strategies that prevent the risk of overfishing strong year classes (Licandeo et al., 2020).

Length and age data form the basis of our understanding of fish population fluctuations in abundance, age structure, or demographic parameters (e.g., growth and mortality rates). Fish length and age data are routinely obtained from hard parts such as fin rays, scales, and especially otoliths. These calcified structures have the property of growing continuously over the life of the fish in correlation with somatic growth. Otoliths form growth increments with an annual periodicity that allows precise age estimation of the fish (Campana, 2001; Casselman, 1987). The annual increments of the otoliths have also been used to backcalculate individual size at earlier ages, allowing the reconstruction of past growth trajectories of fish (Francis, 1990). Backcalculation methods have the advantage of providing growth information on early-life stages that may be underrepresented due to sampling constraints (Vigliola & Meekan, 2009). Fitting growth models (e.g., von Bertalanffy [VB]) to length-at-age data allows for comparative analysis of growth parameters among regions, populations, sex, or cohorts (Campana et al., 2016; Saborido-Rey et al., 2004), and the identification of growth drivers at the population level (Brunel & Dickey-Collas, 2010; Sinclair et al., 2002).

The analysis of individual-level variation in fish growth through linear mixed-effects models is an approach that complements studies on population-level response to environmental change. This approach allows the width of a given annual increment to be analysed as a function of individual intrinsic factors (i.e., sex and age) and extrinsic factors (i.e., physicochemical parameters, intra- and interspecific interactions) that occur at the time of its formation (Morrongiello & Thresher, 2015; Weisberg et al., 2010). The approach of biochronology through linear mixed-effects models constitutes a valuable tool for estimating variation in fish growth and its underlying causes, over century-long (Denechaud et al., 2020; Smoliński et al., 2020) or shorter periods (van der Sleen et al., 2018).

In the Gulf of St. Lawrence (GSL), Canada, significant modifications in environmental conditions and ecosystem structure have occurred over the past decades. The GSL is characterized by increasing temperatures and increasing bottom-layer hypoxia, attributable to the decrease in cold and oxygen-rich Labrador Current water inflow in favor of the warm, oxygen-poor Gulf Stream water entering the GSL through Cabot Strait (Blais et al., 2021; Galbraith et al., 2021). These environmental changes have resulted in an alteration in species composition characterized by the collapse or resurgence of several exploited fish stocks (Bourdages et al., 2022; DFO, 2021; Senay et al., 2021). The case of deepwater redfish (*Sebastes mentella*) is a compelling example of drastic fluctuations in the biomass of fish populations in the GSL. This long-lived, late-maturing species (reaching maturity around age 10, Gascon, 2003, and living up to 75 years, Campana et al., 1990) is characterized by spasmodic recruitment, with stock biomass supported by strong year classes produced decades apart (Caddy & Gulland, 1983). In the GSL stock, the strong year classes from the early 1980s supported the fishery captures until a moratorium was declared in 1995. After nearly three decades of low abundance, the GSL stock is now experiencing a massive recovery due to unprecedentedly high recruitment events in 2011–2013, estimated to be five times stronger than those in the early 1980s. This remarkable resurgence has led to the announcement of the reopening of the commercial fishery in 2024. Given the spasmodic nature of the recruitment of redfish, strong year classes are central to both GSL population resilience and persistence. The sustainability of the fishery thus also relies heavily on strong year classes, emphasizing the importance to understand the drivers of growth variation before exploitation. In addition, the 1980s and 2010s year classes emerged under contrasting oceanographic and ecological constraints, offering a unique opportunity to understand the drivers of growth.

In the present study, otoliths were used as annual growth recorders to investigate changes in population-level and individual-level growth in GSL redfish by focusing on the strong year classes of the early 1980s and early 2010s. First, length at age was backcalculated from individuals born in these periods to test the hypothesis that the exceptionally strong year classes from the early 2010s experienced growth reduction due to density-dependent pressures. Second,

we built a chronology of otolith annual increment width and designed mixed-effect models to partition the impact of intrinsic and extrinsic drivers of redfish growth variation. Emphasis was placed on testing the hypothesis of density-dependent and temperature control.

2 | MATERIALS AND METHODS

2.1 | Sample collection

The present study specifically targeted the last two strong recruitment events (1980–1981 and 2011–2013) in *S. mentella*, one of the two *Sebastes* species that compose the redfish stock of the GSL. The Atlantic redfish, *S. mentella*, and the Acadian redfish, *Sebastes fasciatus*, present almost indistinguishable morphologies and have historically been exploited and managed without differentiation (DFO, 2022). After exceptional recruitment in 2011–2013, *S. mentella* largely dominates the GSL stock, with an estimated biomass reaching 3.2 million tons, representing more than 80% of the total demersal biomass estimated by Fisheries and Oceans Canada (DFO) (DFO, 2022; Senay et al., 2021). Redfish sampling was carried out in the northern GSL during the annual multidisciplinary scientific bottom-trawl survey conducted every summer since 1984 by DFO (Bourdages et al., 2003). The early 1980–1981 year classes were sampled during the summer of 1987 by bottom-trawl survey aboard the M.V. *Lady Hammond* using a Western IIA bottom trawl. The 2011–2013 year classes were sampled during the 2016 and 2018 summers on board the CCGS *Teleost* equipped with a Campelen 1800 bottom trawl. Individuals from strong year classes were targeted at sizes ranging between 19 and 24 cm (age 6–7 years) and between 16 and 23 cm (age 5–7 years), respectively, for the early 1980s and 2010s cohorts. Sex was determined, and immature fish were excluded from the assessment of growth drivers to minimize the potential effects of maturation on somatic growth. Anal-fin rays were counted to differentiate *S. mentella* from *S. fasciatus* within the dataset (Senay et al., 2022). In the absence of genetic identification, the number of anal-fin rays remains the main criterion used by DFO to differentiate the two species (anal-fin rays ≥8 for *S. mentella* and ≤7 for *S. fasciatus*). However, this species identification technique still has a nonnegligible bias compared to genetic identification (e.g., malate dehydrogenase locus [MDH-A*]), estimated at more than 10% (Senay et al., 2022), and we thus cannot exclude the possibility that individuals of *S. fasciatus* were included in the analysis. A total of 384 individuals (102 from the 1980s and 282 from the 2010s) were assigned to *S. mentella* and considered for population growth parameter estimation and the analysis of growth drivers in redfish population from the GSL.

2.2 | Ethics statement

Ethical review and approval was not required because the study was conducted in the field using animals killed during DFO scientific surveys.

2.3 | Otolith preparation

Redfish right sagittal otoliths were extracted, cleaned of organic tissues, rinsed and dried under a laminar flow flume hood before being embedded in epoxy resin (Miapoxy 100 and Miapoxy 95 [4:1], Freeman, OH, USA). Otoliths were transversely sectioned (600 µm thick on average) through the core with a slow-speed diamond-bladed saw (IsoMet saw, Buehler, IL, USA) using ultrapure water as coolant and lubricant. Transverse sections were polished using three grades of aluminum oxide polishing (1200-µm grade, 3M) and lapping films (1- and 5-µm grade, 3M) and mounted on petrographic slides with thermoplastic glue (Crystalbond 509; Aremco Products, NY, USA).

2.4 | Age estimation and growth measurements

Seasonal formation of annuli has previously been validated in *S. mentella* (Campana et al., 1990; Nedreaas, 1990). In the present study, redfish age estimations were obtained from otolith transverse section images taken under reflected light using a Leica M125C stereomicroscope coupled with the Leica MC 170 HD-A microscope camera. An annual increment was defined as the succession of a translucent growth zone and an opaque growth zone corresponding to alternated periods of slow and rapid growth. We proceeded by first measuring the otolith radius at capture and placing reading marks on the external border of each opaque zone. Increment widths were measured on the ventral axis of the otolith, from the core to its edge. ImageJ software (Schneider et al., 2012) and ObjectJ plugin (https://sils.fnwi.uva.nl/bcb/objectj/) were used to annotate the images and take the measurements. The use of otolith increment width as a proxy for somatic growth in redfish from the GSL was confirmed by the correlation of otolith radius with fish length (Figure S1).

2.5 | Backcalculated growth

The backcalculation of individual length at age was performed based on the scale proportional hypothesis (SPH) that was considered the best fitting model. This evaluation was based on a visual inspection of the general shape of the curve. We also compared the length-at-age estimations to other models, including the Dahl–Lea, Fraser–Lee, and the body proportional hypothesis (Ogle, 2013a). The equation of the SPH model (Francis, 1990) is as follows:

$$L_i = S_i/S_c(L_c + a/b) - a/b \quad (1)$$

where L_c and S_c, respectively, represent the length of the fish and the radius of the calcified structure at the time of capture. L_i and S_i represent the length of the fish and the radius at age i on the calcified structure. The intercept $-\frac{a}{b}$ passes through each observed (S_c, L_c) point.

2.6 | VB growth parameter estimation

To compare the growth rates between individuals from the 1980s and the 2010s, a VB growth model was fitted to the backcalculated length-at-age data, which is typically applied to redfish growth data (Campana et al., 2016; Stransky et al., 2005). For this, we used the *FSA* R package (Ogle et al., 2023). The process first aimed to find the starting values (L_{inf}, K, and t_0) using the Ford and Walford method (*vbStarts* function). The parameters and their confidence intervals were then estimated using a bootstrap procedure (*nslBoot* function, 999 iterations). We also calculated the omega coefficient ω, $\omega = k \times L_{inf}$, which is considered a good representation of the early-life growth rate (mm yr^{-1}) near t_0 (Gallucci & Quinn, 1979). Differences in the parameters of the VB growth model between the periods were tested by computing Akaike criterion corrected for small sample size (AICc) to determine the best-fitted model following the approach outlined by Ogle (2013b). A general model that includes separate parameter estimates for individuals from the 1980s and 2010s year classes was compared with several other models that assume common parameters between the two periods (Table S1). It is worth noting that the limited size range of the captured individuals may lead to an underestimation of the L_{inf} parameter. However, because we are considering individuals of similar size between the early 1980s and 2010s year classes, the comparison of the VB growth parameter between the two periods is not affected by the limited size range.

2.7 | Selection of predictors for mixed-effect models

The intrinsic and extrinsic parameters considered as explanatory factors for redfish growth variation, here represented by variation in otolith increment width, are represented in Table 1. Intrinsic variables comprise age at increment formation (age), age at capture (AAC), and sex (sex). We also considered the variable FishID, which is a unique identifier assigned to each individual. Year of increment formation (year) and year class (cohort) were also implemented in the analysis.

The extrinsic drivers were environmental, either physicochemical (i.e., water temperature, dissolved oxygen concentration, and temperature of the cold intermediate water layer [CIL]), demographic (e.g., redfish *Sebastes* spp. biomass), or biological (e.g., redfish prey abundance or biomass).

The average annual temperature for different layers was obtained from the DFO annual research document on physical oceanographic conditions in the GSL (Galbraith et al., 2021). Because redfish migrate to deeper waters as they grow (Atkinson, 1984; Gascon, 2003; Senay et al., 2021), we considered four temperature parameters: sea-surface temperature and temperatures at three different depths (150, 200, and 300 m).

We also tested the annual average temperature and volume of the CIL obtained from the DFO annual research document on physical oceanographic conditions in the GSL (Galbraith et al., 2021). The CIL is a <1°C water layer found in the GSL at a depth interval ranging

TABLE 1 Description and data range of parameters used in the mixed-effects model design for the analysis of GSL redfish (*Sebastes* sp.) growth.

Parameter	Description	Variable type	Data range
Increment	Width of increment (μm)	Response	1982–1987 and 2013–2018
FishID	Unique identifier number	Random	
Year class	Group of individuals born the same spawning season	Random	
Year	Year of increment formation	Random	
Age	Age at increment formation	Fixed, random	
AAC	Age at capture	Fixed	
Sex	Sex of the individual	Fixed	
SST	May to November average sea-surface temperature (°C)	Fixed	1982–1987 and 2013–2018
T_300	300 m depth temperature (°C)	Fixed	1982–1987 and 2013–2018
T_200	200 m depth temperature (°C)	Fixed	1982–1987 and 2013–2018
T_150	150 m depth temperature (°C)	Fixed	1982–1987 and 2013–2018
CIL_T	Cold intermediate layer temperature (°C)	Fixed	1982–1987 and 2013–2018
CIL_V	Cold intermediate layer volume ($\times 10^3$ km^3)	Fixed	1985–1987 and 2013–2018
O_300	300 m depth dissolved oxygen concentration (μM)	Fixed	2013–2018
Shrimp_Biomass	Northern shrimp *Pandalus borealis* annual biomass (kg/km^2)	Fixed	2013–2018
Redfish_Biomass	*Sebastes* spp. annual biomass (10^3 tons)	Fixed	1984–1987 and 2013–2018
C_hyperboreus	*Calanus hyperboreus* annual abundance ($\times 10^3$ individual m^{-2})	Fixed	2013–2018
C_finmarchicus	*Calanus finmarchicus* annual abundance ($\times 10^3$ individual m^{-2})	Fixed	2013–2018

Abbreviation: GSL, Gulf of St. Lawrence.

between 30 and 120 m, which results from the melting of the winter ice cover (Gilbert & Pettigrew, 1997). The CIL temperature is likely to have an impact on the survival of redfish larvae that must migrate through the CIL during their development (Burns et al., 2022; Gascon, 2003). The volume and thermal properties of the CIL are also suspected of playing a role in zooplankton abundance and phenology (Blais et al., 2021).

The last environmental parameter tested was the annual average concentration of dissolved oxygen in the deep layer of the GSL (300 m depth) obtained from the DFO annual research document on chemical and biological oceanographic conditions in the estuary and GSL (Blais et al., 2021). Dissolved oxygen depletion in the deep water of the estuary and GSL has been exacerbated in recent decades, with some areas that have been identified as hypoxic (Blais et al., 2021). This phenomenon is recognized to have a negative impact on several species of fish and invertebrates of the GSL ecosystem (e.g., negative impact on Greenland halibut metabolism, Pillet et al., 2016; loss of habitat for the northern shrimp, Bourdages et al., 2022).

We investigated the potential density-dependent effect on growth by integrating the demographic parameter of the total biomass of redfish (*Sebastes* spp.) (considering both mature and immature fish), obtained from the DFO redfish stock assessment document (DFO, 2022). Including biomass from both mature and immature fish allows us to account for the density-dependent effects on growth resulting from cannibalism of larger redfish (>30 cm) toward smaller redfish in addition to intraspecific competition for resources.

Finally, to test the influence of prey abundance on growth, we considered the abundance (individuals m^{-2}) of two copepod species, *Calanus finmarchicus* and *Calanus hyperboreus*, as well as the biomass (kg km^{-2}) of the northern shrimp, *Pandalus borealis*, as they represent the main prey for small (<20 cm) and larger redfish (>20 cm), respectively (Brown-Vuillemin et al., 2022, 2023). Copepod and shrimp abundance data were obtained from Blais et al. (2021) and Bourdages et al. (2022), respectively. It should be noted that although redfish can be cannibalistic, we did not consider redfish biomass as a proxy for prey abundance because cannibalism occurs only in large redfish (>30 cm), which are not considered in the present study. The time series of environmental parameters tested in the mixed-effects models is shown in Figures S2 and S3.

2.8 | Mixed-effects model of redfish growth

Following the approach developed by Morrongiello and Thresher (2015) based on the work of Weisberg et al. (2010), we designed a series of mixed-effects models using variable fixed and random structures to show the influence of intrinsic and extrinsic sources of variation in redfish otolith increment width, a proxy for somatic growth. Before the mixed-effects models design, the variables increment (increment width), age, and AAC were log transformed to meet model assumptions. Extrinsic predictors were mean centered and scaled to facilitate model convergence and interpretation of interaction terms (Morrongiello & Thresher, 2015). The width of increments 2–7 was included in the mixed-effects model design. The number of increment measurements per year of formation and year class is shown in Figure S4. Following Smoliński et al. (2020), the first increment was excluded from mixed-effects analysis because it does not represent a complete year of life but corresponds to the timing from larval extrusion to the first winter. The relationships between the environmental parameters identified in the best mixed-effects models and the width of the first increment averaged by year of formation were tested using Pearson's correlations after normality and homoscedasticity assumptions were validated (Figure S5).

First, we determined the optimal base model that included the full intrinsic structure (age, AAC, and sex) and introduced a combination of random intercept and slope (Table S2). A random intercept for FishID was included to account for (1) repeated measurement structure of increment measurements and (2) interindividual variation in growth. Random intercepts for year and cohort were added to, respectively, test for correlation among the width of the increments deposited in the same year and correlation among the width of increments from individuals belonging to the same year class. The inclusion of a random *age* slope for FishID in mixed models accounts for the individual level of variability in age-related growth rate (Morrongiello & Thresher, 2015). The benefit to model performance of adding random *age* slope for *year* and random *age* slope for *cohort* to account for variable growth-year or variable growth-cohort relationships among individuals was also examined. AICc (Burnham & Anderson, 2004) was used in every step of the model design to rank the tested models and select the optimal one. We also used ΔAICc for model comparison, which is the difference between each model's AICc and the lowest value. At this step of model optimization, the best linear unbiased predictors (BLUP) were extracted from the model with the lowest AICc that included only year random effect (model MR2) to visualize the interannual variation in redfish growth over the period covered by the analysis (Morrongiello & Thresher, 2015). We also represented the cohort-specific variation in growth by extracting the BLUPs from the model with the lowest AICc, including only the cohort random effect (model MR3).

Second, the optimal random-effects structure identified in the first step was used to determine the best intrinsic fixed-effects model among *age*, AAC, *sex*, and a combination of these factors to account for possible age and sex-specific variability in growth rates. In the third step, extrinsic factors were introduced to model optimization. The time series covered by either environmental, biological, or demographic parameters was different, which constrained us to develop two different mixed-effects models for two time periods. The first model tested the influence of temperature at different depths (surface, 150, 200, and 300 m), temperature of the cold intermediate layer, and redfish biomass on redfish growth for the period between 1982–1987 and 2013–2018. The second model was run for the recent period of 2013–2018 for which other extrinsic factors as the effect of prey abundance/biomass and dissolved oxygen concentration could be added and tested. For performance comparison,

models were fitted with the maximum likelihood estimated error. The optimal model (lowest AICc) was then refitted with restricted maximum likelihood estimates of error to provide unbiased parameter estimates (Zuur et al., 2009). *p*-Values for the fixed-effects were obtained using Satterthwaite's approximation for degrees of freedom, implemented using the lmerTest from *lme4* package (Bates et al., 2015) from the Rstudio software (R Core Team, 2020). AICc comparisons were carried out using the *AICcmodavg* (Mazerolle, 2020) and *MuMin* (Bartón, 2023) packages.

2.9 | Redfish annual growth trajectories

Given the importance of early growth performance on growth potential in later life stages (e.g., carryover effect; O'Connor et al., 2014), we analysed the growth trajectory of year classes from the 1980s and the 2010s using autocorrelation analysis of otolith increment width. For this purpose, Pearson's correlation coefficients were calculated between the widths of the increments formed at each age. The correlation coefficients were presented in surface plots, respectively, for year classes from the 1980s and the 2010s.

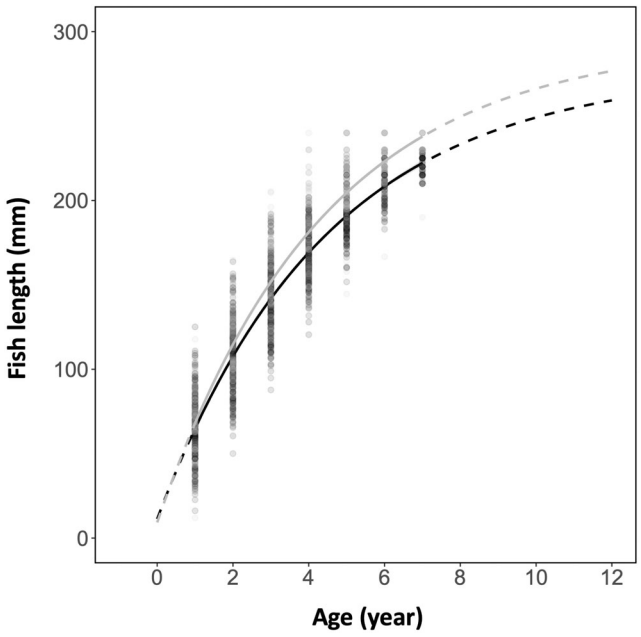

FIGURE 1 Redfish (*Sebastes* sp.) growth curve based on backcalculated length at age from otoliths for 1980s year classes in gray and 2010s year classes in black. Solid lines and dashed lines represent the fitted curve, respectively, for the observed and for the predicted range of ages.

3 | RESULTS

3.1 | VB growth parameters

Individuals from the 1980s strong year classes were larger than individuals from the 2010s (average length of 22.6 ± 1.4 cm for the 1980s vs. 20.1 ± 1.8 cm for the 2010s), although age estimation from analysis of otolith structure revealed that individuals had approximately similar ages (5.7 ± 0.96 vs. 5.3 ± 1.2 years). This observation suggests that individuals from the 1980s grew faster than those from the 2010s. This was supported by the estimates from the VB growth model on GSL redfish backcalculated size at age (Figure 1). Comparison of the VB growth curves and growth parameters between the two periods revealed that individuals from the 1980s presented a higher asymptotic size (L_{inf}), a higher growth rate (K), and a higher growth rate in early-life stage (θ) (Table 2). However, the difference was significant only for L_{inf}.

3.2 | Best mixed-effects model design

In the design of the best mixed-effect modeling of GSL redfish growth, the best random-effects structure identified by AICc was a random intercept for the *year* parameter and both a random intercept and an *age* slope for FishID (Table S2, model MR2). The best model supported by the lowest AICc for the intrinsic terms integrated *age* and AAC terms (Table S3, model MI4). The associated marginal R^2 of 0.30 indicated that the fixed effects explained 30% of the variation in redfish growth. With a conditional R^2 of 0.50, the entire model (both fixed and random structures) explained 50% of the observed variation in growth. Among the four different temperature parameters, T_300 and T_200 best explained redfish growth for the longest time series and for recent years, respectively (Table S4). According to the AICc criterion, the final optimal model for studying redfish growth variation between the 1980s and the 2010s was model M6 (Table S5). The fixed extrinsic structure considered in model M6 was the redfish biomass *Sebastes* spp. and temperature of the cold intermediate layer (CIL_T). The addition of extrinsic factors to the model design increased the explained variance to 52% (Table 3). For the 2010s, the best model with the lowest AICc was model M9 and included redfish biomass as the only

TABLE 2 Number of individuals, mean length (±SD), mean age (±SD), von Bertalanffy growth model parameters, and associated SE (SE) for redfish (*Sebastes* sp.) 1980s and 2010s year classes.

Year classes	N	Mean length	Mean age	L_{inf}	SE	K	SE	t0	SE	θ
1980s	100	226.1 ± 13.61	5.65 ± 0.96	295.15	13.32	0.23	0.02	−0.14	0.08	68.35
2010s	269	200.9 ± 17.74	5.27 ± 1.2	277.22	6.90	0.22	0.01	−0.19	0.05	62.54

TABLE 3 Variance component and parameter estimates describing growth variation in redfish (*Sebastes* sp.) for (a) the best mixed-effects model M6 for 1980s and 2010s, (b) the best mixed-effects model M9 for 2010s, and (c) the second best mixed-effects model M10 for 2010s.

(a)	**Model M6**	***Nobs* = 1535, *Nind* = 369, *Nyear* = 10**				
	Random effects		**Variance**	**SD**	**Correlation**	
	FishID	(Intercept)	0.09	0.31		
	Age|FishID		0.06	0.24	−0.91	
	Year	(Intercept)	0.0005	0.02		
	Residuals		0.07	0.27		
	Fixed effects	**Estimate**	**SE**	***df***	***t*-value**	***p*-value**
	(Intercept)	5.92	0.05	181.20	110.97	**<0.001**
	Age	−0.40	0.04	36.73	−8.99	**<0.001**
	AAC	−0.38	0.08	138.57	−4.46	**<0.001**
	Redfish biomass	−0.06	0.02	21.76	−3.49	**0.0021**
	CIL_temp	−0.02	0.01	10.70	−1.46	0.1733
	Conditional R^2	0.52				
	Marginal R^2	0.34				
(b)	**Model M9**	***Nobs* = 1152, *Nind* = 270, *Nyear* = 6**				
	Random effects		**Variance**	**SD**	**Correlation**	
	FishID	(Intercept)	0.10	0.32		
	Age|FishID		0.07	0.26	−0.91	
	Year	(Intercept)	0.0002	0.02		
	Residuals		0.07	0.26		
	Fixed effects	**Estimate**	**SE**	***df***	***t*-value**	***p*-value**
	(Intercept)	5.85	0.06	118.30	92.75	**<0.001**
	Age	−0.33	0.05	15.62	−6.30	**<0.001**
	AAC	−0.44	0.09	82.75	−5.00	**<0.001**
	Redfish biomass	−0.09	0.02	8.42	−4.74	**0.0013**
	Conditional R^2	0.55				
	Marginal R^2	0.37				
(c)	**Model M10**	***Nobs* = 1152, *Nind* = 270, *Nyear* = 6**				
	Random effects		**Variance**	**SD**	**Correlation**	
	FishID	(Intercept)	0.10	0.32		
	Age|FishID		0.07	0.26	−0.91	
	Year	(Intercept)	0.0002	0.01		
	Residuals		0.07	0.26		
	Fixed effects	**Estimate**	**SE**	***df***	***t*-value**	***p*-value**
	(Intercept)	5.87	0.07	344.86	88.62	**<0.001**
	Age	−0.38	0.07	400.39	−5.46	**<0.001**
	AAC	−0.38	0.10	327.50	−3.83	**<0.001**
	T_200	0.03	0.02	10.03	1.16	0.2747
	Redfish biomass	−0.06	0.03	107.80	−2.50	**0.0139**
	Conditional R^2	0.55				
	Marginal R^2	0.37				

Note: Significant *p*-values are presented in bold font.
Abbreviations: AAC, age at capture; CIL, cold intermediate water layer.

fixed extrinsic parameter. The second-best model M10, which included both temperature at 200-m depth and redfish biomass, had a ΔAICc very close to that of M9 and was therefore considered for interpretation. The two models had a similar R^2 of 0.55, indicating that 55% of the variation in redfish growth was explained by their fixed and random structures.

3.3 | Growth variation

The extracted BLUPs for the *year* random effect allowed us to visualize interannual variation in growth (Figure 2). Annual growth was higher on average for the 1980s year classes than for the 2010s year classes. Larger increments were observed in 1986 and 2015. The annual growth was predicted to be the lowest for 2018. BLUPs for *cohort* random effect showed that the 1980, 1981, and 1982 year classes presented larger increment widths and that the 2012 and 2013 year classes presented the smallest.

3.4 | Intrinsic source of variation in growth

All factors combined, *age* at increment formation was the main factor responsible for growth variation for both M6 and M9 models. Increment widths gradually declined as individuals aged. We observed a negative relationship between redfish growth and ACC, and individuals captured at older ages presented lower growth. There was also significant individual variability in growth as demonstrated by the relatively high proportion of variance explained by FishID.

3.5 | Extrinsic source of variation in growth

The final model M6 designed to investigate the drivers of growth for the longest time series available reported that redfish biomass presented a significant negative relationship with redfish growth (p-value = 0.002) (Table 3). Within the range of redfish biomass observed for the period, model M6 predicted a decrease in growth of 17.68% (Table 4; Figure 3). The temperature of the CIL was the

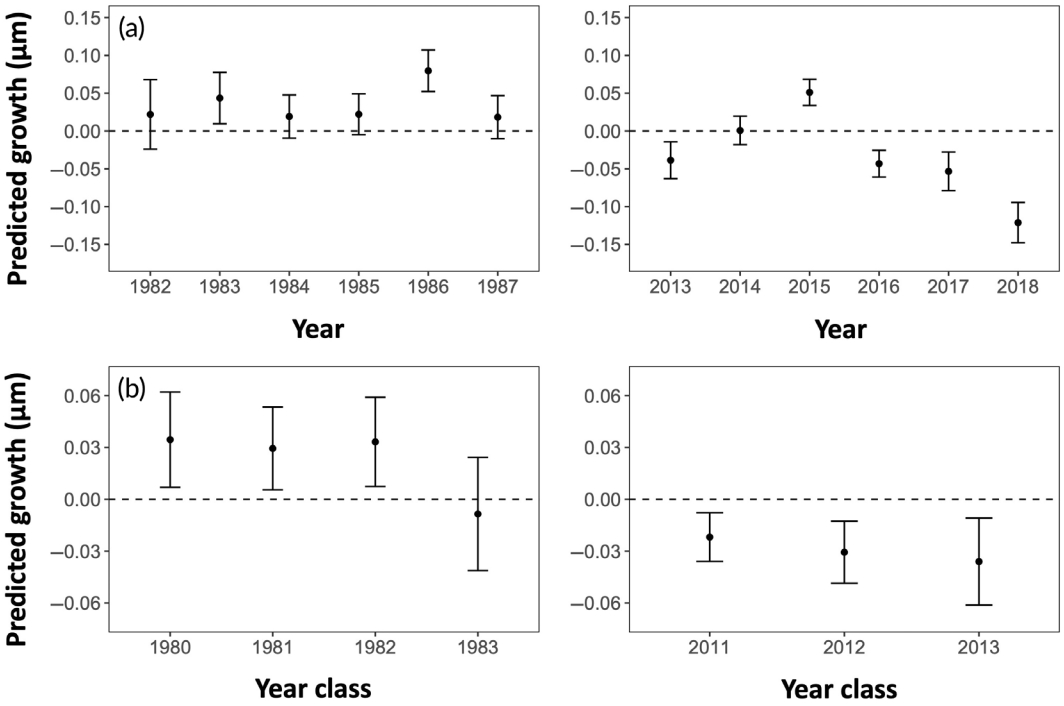

FIGURE 2 Redfish (*Sebastes* sp.) predicted (a) interannual variation in growth and (b) between cohort variation in growth, represented by best linear unbiased predictors (BLUP ± SE), respectively, based on year random effect estimates from model MR2 and cohort random effect estimates from model MR3.

TABLE 4 Predicted percentage of change in redfish (*Sebastes* sp.) growth with extrinsic factors from best mixed-effects models.

Mixed-effect model	Extrinsic factor	Predictor range	Predicted % of change in growth
Model M6	Redfish biomass	170–3000 Kilotons	−17.68
1982–1987 and 2013–2018	CIL temperature	−0.9 to 0.1°C	−6.81
Model M9	Redfish biomass	170–3000 Kilotons	−23.72
2013–2018			
Model M10	Redfish biomass	170–3000 Kilotons	−18.43
2013–2018	200 m depth temperature	4.9–5.6°C	5.12

Abbreviation: CIL, cold intermediate water layer.

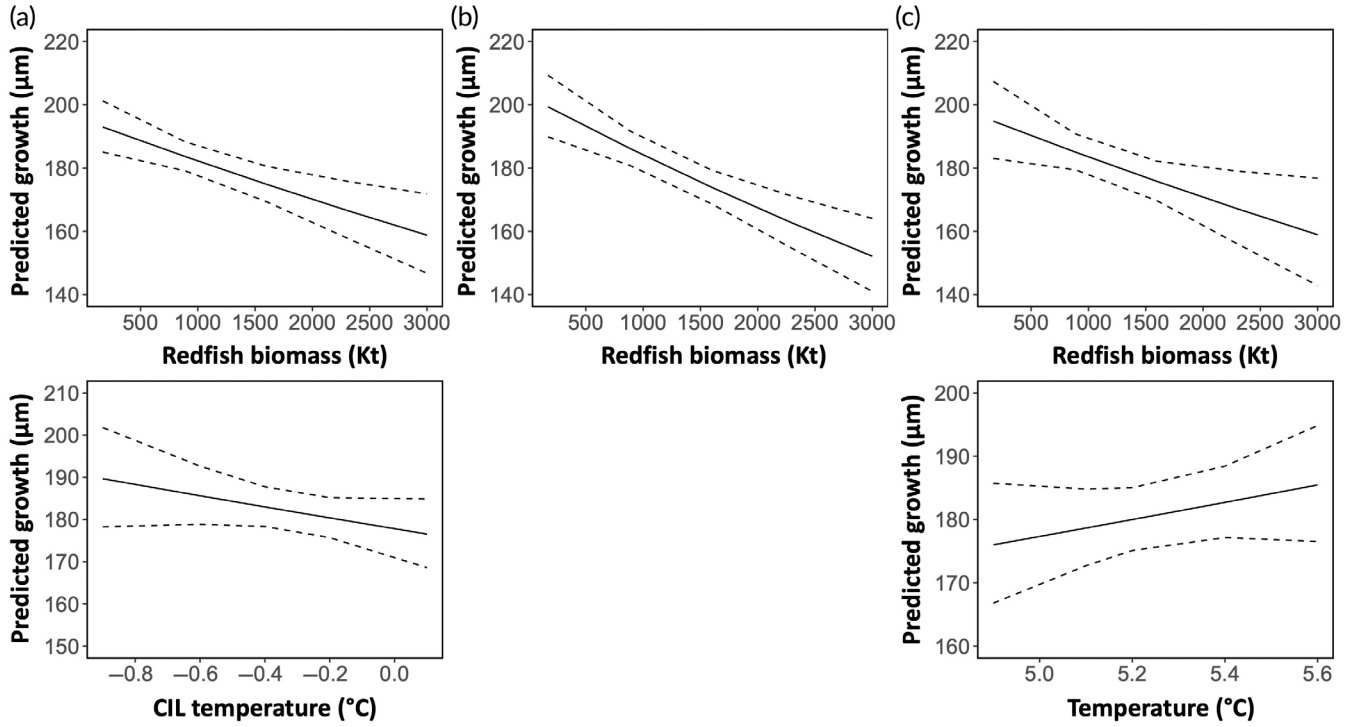

FIGURE 3 Predicted effects of environmental variables on redfish (*Sebastes* sp.) growth (a) from model M6, (b) from model M9, and (c) from model M10. The dotted lines represent 95% CI.

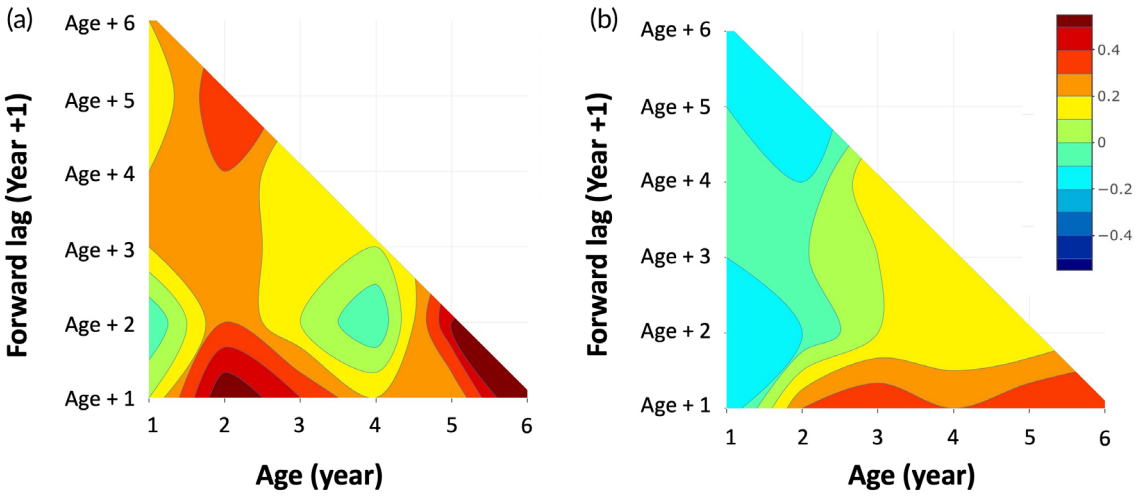

FIGURE 4 Pearson's correlation coefficients between increment width relative to age of formation and the width of the next annual increment formed at age + 1, age + 2, ..., age + *n* for redfish (*Sebastes* sp.) (a) 1980s year classes and (b) 2010s year classes.

second extrinsic factor that was kept by the AICc in model M6, although it was not significant (p-value = 0.17). Growth was predicted to decrease by 6.81% with increasing temperature of the CIL (within the range of experienced CIL temperature values). Nevertheless, a significant negative correlation was found between CIL temperature and first increment width ($r = -0.9$, p-value = 0.0004).

In recent years (2013–2018, model M9), redfish biomass has remained one of the main extrinsic drivers of redfish growth (p-value = 0.0013), with a predicted decrease in growth of 23.72%. The second best AICc model M10 retained temperature at 200-m depth that was not significant (p-value = 0.27) but presented a positive relationship with growth. Model M10 predicted a 5.12% increase in growth with warming temperatures and a decrease in growth of 18.43% with increasing stock biomass.

There was no significant correlation between the first increment width and any of the temperature parameters identified in the mixed-effect models (200 m: $r = 0.14$, p-value = 0.7674; 300 m: $r = -0.08$, p-value = 0.8389).

3.6 | Redfish annual growth trajectories

Autocorrelation analysis using Pearson's correlation of otolith annual increment widths indicated district average growth trajectories between the 1980s strong year classes and the exceptional 2011–2013 year classes (Figure 4). Individuals from the 1980s year classes generally exhibited a positive correlation between increment widths since the first year of life. Only one exception is noted, with the weak negative correlation observed for increments 4 and 5. For individuals belonging to the 2010s year classes, positive correlations were detected after age 3, whereas the previous increment widths were negatively correlated.

4 | DISCUSSION

The present study provides new perspectives on intrinsic and extrinsic drivers of growth variation in GSL redfish during the strong recruitment events that emerged under contrasting biotic and abiotic conditions in the 1980s and 2010s. A comparison of VB growth parameters derived from backcalculated individual length at age revealed slower growth rates and smaller sizes at age in the 2010s relative to the 1980s. Density dependence was identified as the main determinant driving growth variation between the two periods. The notable increase in temperature in the GSL system from the 1980s to the 2010s was associated with both positive and negative effects on redfish growth. Growth was positively linked to increasing temperatures of the deep layer of the water column, where individuals settle at the preadult stage. However, a negative relationship between growth and increasing temperature in the cold intermediate layer was observed. Rather than being attributable to a direct effect of CIL temperature on redfish growth, this observation could be explained by the negative relationship between the abundance of the copepod *C. hyperboreus*, one of the main prey of early juvenile redfish (Brown-Vuillemin et al., 2022; Brown-Vuillemin et al., 2023), and CIL temperature (Blais et al., 2021). Finally, the analysis of growth trajectories through increment autocorrelation highlighted the importance of a carryover effect in the growth potential of strong year classes of redfish.

4.1 | Density-dependent feedback on growth

Challenging the paradigm that density-dependent effects on survival outweigh density-dependent effects on growth in fish populations (Lorenzen, 2008; Lorenzen & Enberg, 2002), several studies have emphasized that density dependence in growth is more frequent than expected and often occurs in conjunction with density dependence in recruitment (Lorenzen & Enberg, 2002; Zimmermann et al., 2018). Ecologically, density-dependent growth during the juvenile and adult stages of fish results from the reduction in individual feeding success through intraspecific competition for prey (Beverton & Holt, 1957; Lorenzen & Enberg, 2002). Zimmermann et al. (2018) revealed that population regulation in several species of the genus *Sebastes* represents a case where density-dependent growth during the preadult and adult stages can overcome the density-dependent effects on survival during early life. The importance of density-dependent mechanisms in regulating growth could be attributable to the fact that *Sebastes* species are typically characterized by spasmodic recruitment, leading to the extreme dominance of a single strong year class within the stock at the decadal scale (DFO, 2022; Licandeo et al., 2020). An inverse relationship between growth rate and year-class strength has been documented in several species of the genus *Sebastes* (Saborido-Rey et al., 2004).

Results from our model combined with estimated growth trajectories indicated that growth variation among strong year classes in GSL redfish was primarily driven by stock density and likely resulted from very high competition for food. It is worth noting that the lack of monitoring of abundance or biomass indices of other key zooplankton and invertebrate prey species in the GSL (e.g., the amphipod *Themisto* sp., the pink shrimp *Pasiphaea multidentata*, Brown-Vuillemin et al., 2022) likely prevented us from capturing the full effect of prey availability on redfish growth. Recruitment of *S. mentella* from the GSL in the early 2010s was of unprecedented level relative to any other recruitment event since the stock has been monitored, including the strong year classes from the early 1980s (DFO, 2022). After the onset of the strong 2011–2013 year classes, redfish reached a record estimated biomass of 4.4 million tons in 2019, representing about 90% of the total biomass sampled in the annual DFO bottom-trawl survey (DFO, 2022). In comparison, the 1988 redfish biomass, which followed the 1980–1981 year classes, was more than five times lower, estimated to be ~800,000 tons (DFO, 2022).

The extreme nature of the recruitment event of the 2010s likely exacerbated density-dependent feedbacks, which were more evident than in the 1980s. In a study of redfish diet composition over three decades, Brown-Vuillemin et al. (2022) noted the emergence of cannibalism in the 2010s as a response to the onset of the strong year classes. Cannibalism is considered a significant regulator of fish population density (Ricker, 1954; Smith & Reay, 1991), and its occurrence has been documented in several populations experiencing high conspecific density (reviewed by Pereira et al., 2017). In the case of GSL redfish, the sudden increase in cannibalism was interpreted as a density-dependent response in the context of rapidly decreasing shrimp abundance (Bourdages et al., 2022; Brown-Vuillemin et al., 2022). In addition to the change in diet composition, a significant decrease in size at maturity was observed in individuals from the 2011 to 2013 year classes (DFO, 2022), a characteristic often attributed to suboptimal growth (Trippel, 1995). Histological examination of the gonads in individuals of *S. mentella* from the recent strong year classes revealed a reduction in the size at which 50% of individuals are mature (L_{50}) from 21.7 to 18.1 cm for males and from 23.6 to 19.2 cm for females (Brûlé et al., 2024; DFO, 2022). These changes in diet composition and size at maturity suggest that the slow growth associated with the extreme abundance of the recent 2011–2013 cohorts was due to strong competition pressure for prey resources.

The strength of the density-dependent feedback on growth will likely increase as the 2011–2013 year classes mature. This is

attributed to the projected further decline in the biomass of redfish preferred prey, the northern shrimp (*P. borealis*), combined with increased individual energy requirements as the deep waters of the GSL warm (Brett, 1979). In addition, cannibalism is expected to intensify as individuals reach larger sizes and transition to a more piscivorous diet (Brown-Vuillemin et al., 2022), which is likely to affect juvenile redfish survival and limit the emergence of new strong year classes in the midterm. Ultimately, a better mechanistic understanding of the density-dependent dynamics that occur after the emergence of strong year classes would facilitate the development of management strategies designed to maximize the long-term growth potential of the stock (Licandeo et al., 2020).

4.2 | Temperature effect on growth variation

Temperature is recognized as the main driver of growth in marine ectotherms, including fish (Brett, 1979; Jobling, 1996). As the current warming of marine ecosystems on the global scale is predicted to intensify in forthcoming years (Fox-Kemper et al., 2021; IPCC, 2019), determining the effect of temperature on fish growth has become a primary goal of otolith biochronology studies. These investigations have revealed positive (Denechaud et al., 2020), negative (e.g., after exceeding the thermal optimum; Martino et al., 2019), or contrasting (Smoliński et al., 2020) age-dependent responses to temperature. Variability in temperature has also been identified as a key factor regulating North Atlantic groundfish growth and stock dynamics (Swain et al., 2003), including redfish (Devine & Haedrich, 2011).

In the present study, the 2010s otolith chronology revealed that GSL redfish growth positively correlated with temperature in their deepwater habitat, which has undergone rapid warming in the past two decades (Galbraith et al., 2021). Gene expression data on the growth of GSL redfish support our findings of a positive link between growth and temperature (Martínez-Silva et al., 2022). Although increasing temperature is positively linked to growth in redfish, its effect on the production of preferred redfish prey may be the opposite. For example, local stocks of the northern shrimp (*P. borealis*) have been rapidly declining since 2019, which has been attributed to the warming of their habitat combined with predation by redfish (Bourdages et al., 2022; Brown-Vuillemin et al., 2022). In the context of decreasing prey availability, the higher energy requirements to fuel fast growth at high temperatures could explain the relatively slow growth trajectory exhibited by redfish in the 2010s.

Our results also showed that the temperature of the CIL was negatively associated with the growth rate of redfish. The lower growth of redfish in the 2010s coincided with a warmer CIL temperature (mean: −0.1°C during 2012–2018) compared to the 1980s (mean: −0.3°C during 1982–1987). In species that spend part of their life cycle in association with the CIL, such as Atlantic cod, it has been hypothesized that cold CIL temperatures would negatively affect growth, condition and possibly feeding rates of individuals (Dutil et al., 1999; Gilbert & Pettigrew, 1997). In redfish, because juveniles and adults distribute in the relatively warm deep layer and do not associate closely with the CIL, we hypothesize that the observed CIL temperature effect on growth variation operates indirectly through prey availability rather than through direct exposure to cold temperatures. Variability in the temperature and thickness of the CIL determines the extent of habitat available for several cold-water species occurring in the GSL. For example, Blais et al. (2021) and Starr et al. (2002) reported that high biomass of, respectively, the large calanoid *C. hyperboreus* and that of the amphipod *Themisto* sp. was associated with years of cold CIL temperature. Northern shrimp abundance is also dependent on a cold CIL (Le Corre et al., 2021). Given that *C. hyperboreus* and *Themisto* sp., and northern shrimp, respectively, represent the preferred prey of small-sized and midsized redfish (Brown-Vuillemin et al., 2022), future redfish growth potential in the GSL will depend on the cost–benefit balance of habitat suitability under warming waters and intensifying competition for declining prey availability.

4.3 | Intrinsic factors driving variation in growth

The decrease in increment widths with age is a consistent observation in otolith chronology studies and demonstrates the expected decline in fish somatic growth with age. Another interesting observation is the negative correlation between the fixed AAC effect with individual growth rate, which mostly seems to be related to increment width becoming narrower at older ages. The limited age structure of the dataset and the design of the mixed-effect model did not allow speculation on a possible selection process in favor of slow-growing individuals, which would explain why individuals captured at older ages would have exhibited a slower growth rate.

Additionally, the limited age structure and cohort overlapping in our data likely contributed to the relatively small R^2 values observed from the different models, as well as the important residual variance. Including year classes from both high and low abundances in our statistical analysis would likely provide a more robust test of our hypothesis regarding environmental control on redfish growth through density-dependent pressure and temperature. However, we were limited by the spasmodic nature of the GSL redfish recruitment that systematically results in the underrepresentation of year classes characterized by recruitment failure. These weak year classes are too scarce to be quantitatively sampled by a random stratified monitoring survey.

Another notable observation is that among the random factors controlled in the mixed-effects models, the greatest variance in growth was attributable to interindividual variability. We hypothesized that density-dependent pressure in strong recruitment events could explain the high interindividual variability in growth observed in GSL redfish.

4.4 | Importance of carryover effect in redfish growth

In animals, including fish, an individual's growth potential can be determined by past growth performance. This ecological concept,

referred to as the "carryover effect," can be observed between adjacent life stages, through an individual's life, or even across generations (O'Connor et al., 2014). The carryover of growth potential can occur from the early larval stage of fish, which is reflected by strong autocorrelation of individual growth rate (Pepin, 2015), including in *S. mentella* from the GSL (Burns et al., 2021). In general, strong growth autocorrelation is observed under a fast mean growth rate (Tanaka et al., 2023). In year classes from the 1980s, a carryover effect was clearly visible, with individuals characterized by stable growth trajectories shortly after age 1. The fast or slow growth achieved during early stages thus carried over to later life stages.

Interestingly, there was more variability in the growth trajectories of the exceptionally strong 2010s year classes, for which a carryover effect in growth was observed later in life. Before age 3, there was a negative correlation, albeit weak, in the width of successive annuli. The most likely mechanism that explains this negative correlation is density dependence: by following the dynamics of resource availability, individuals can compensate either by accelerating their growth rate to catch up or by slowing the transition between developmental stages to ensure better survival and maintenance of growth potential (Ali et al., 2003; Metcalfe & Monaghan, 2001). In a situation where food is not limiting, it is less likely that an individual characterized by fast initial growth will end up growing slowly later in life. We thus hypothesized that during the exceptional 2011–2013 recruitment events, intense competition for food was responsible for the observed compensation in growth in the early-life stages. The positive carryover effect in growth at a later life stage can be explained by the shift in redfish diet toward larger prey with higher nutritional value (Brown-Vuillemin et al., 2022).

Growth compensation in redfish exceptionally strong year classes was likely accompanied by early maturation, as indicated by a reduction in L_{50} of ~4 cm for both males and females compared to the last strong recruitment event in the 1980s (Brûlé et al., 2024; DFO, 2022). The reduction in growth potential resulted in a significant reduction in the projected asymptotic length of individuals in the recent strong year classes. It is expected that the L_{inf} will not exceed 30 cm, which represents a decrease of almost 10 cm when compared to individuals from the 1980s cohorts (DFO, 2022).

In anticipation of the reopening of the fishery, the recent 2011–2013 year classes should sustain catches until the next episode of strong recruitment in the stock occurs. Our findings are consistent with other recent studies on the status of GSL redfish stock (Brown-Vuillemin et al., 2022; Brûlé et al., 2024; DFO, 2022; Licandeo et al., 2020; Martínez-Silva et al., 2022), which suggests that the growth potential of these strong recent year classes may be destabilized by the significant density-dependent pressures inherent in this spasmodic stock. The current temperature increase, combined with the decreasing oxygen saturation levels observed in the GSL, is likely to exacerbate the density-dependent control on growth through prey depletion and increased energy requirements.

AUTHOR CONTRIBUTIONS

All authors collectively developed the project's objectives and methodology. Lola Coussau performed sample preparation and age estimations. Lola Coussau conducted the statistical analysis and interpretation with additional input from Olivier Morissette, Dominique Robert, and Pascal Sirois. Lola Coussau wrote the first draft of the manuscript. All authors reviewed, made significant contributions to the draft, and granted final approval for publication.

ACKNOWLEDGMENTS

We thank Fisheries and Oceans Canada (DFO) for providing otolith samples. We are also grateful to S. Gagné (UQAC), I. Allie (UQAC), and A.-L. Fortin (UQAC), who assisted with sample preparation, age estimations, and otolith section annotations.

FUNDING INFORMATION

This project was co-funded by Fisheries and Oceans Canada (DFO) and by the Ressources Aquatiques Québec (RAQ) as part of the partnership programme "Return of Groundfish in the Estuary and Northern Gulf of St. Lawrence" supported by the Fonds de recherche du Québec—Nature et technologies (FRQNT) (2020-RS4-265329). Dominique Robert was supported by the Canada Research Chair Program.

ORCID

Lola Coussau https://orcid.org/0000-0002-1032-7395

REFERENCES

Ali, M., Nicieza, A., & Wootton, R. J. (2003). Compensatory growth in fishes: A response to growth depression. *Fish and Fisheries*, *4*(2), 147–190. https://doi.org/10.1046/j.1467-2979.2003.00120.x

Andersen, K. H., Jacobsen, N. S., Jansen, T., & Beyer, J. E. (2017). When in life does density dependence occur in fish populations? *Fish and Fisheries*, *18*(4), 656–667. https://doi.org/10.1111/faf.12195

Atkinson, D. B. (1984). Distribution and abundance of beaked redfish in the Gulf of St. Lawrence, 1976-81. *Journal of Northwest Atlantic Fishery Science*, *5*(2), 189–197. https://doi.org/10.2960/j.v5.a23

Bartón, K. (2023). Package 'MuMIn'. Version, 1.47.5. https://CRAN.R-project.org/package=MuMIn

Bates, D., Mächler, M., Bolker, B., & Walker, S. (2015). Fitting linear mixed-effects models using lme4. *Journal of Statistical Software*, *67*(1), 1–48. https://doi.org/10.18637/jss.v067.i01

Beverton, R. J. H., & Holt, S. J. (1957). On the dynamics of exploited fish populations. Fishery Investigations, London, Series II. 19, 1–533.

Blais, M., Galbraith, P. S., Plourde, S., Devred, E., Clay, S., Lehoux, C., & Devine, L. (2021). Chemical and biological oceanographic conditions in the estuary and Gulf of St. Lawrence during 2020. Fisheries and Oceans Canada Canadian Science Advisory Secretariat, Research Document 2021/060. pp. iv + 67.

Bourdages, H., Archambault, D., Morin, B., Fréchet, A., Savard, L., Grégoire, F., & Bérubé, M. (2003). Résultats préliminaires du relevé multidisciplinaire de poissons de fond et de crevette d'août 2003 dans le nord du golfe du Saint-Laurent. Secrétariat canadien de consultation scientifique de Pêche et Océans Canada, Document de recherche 2003/078.

Bourdages, H., Roux, M.-J., Marquis, M. C., Galbraith, P., & Isabel, L. (2022). Assessment of northern shrimp stocks in the estuary and Gulf of St. Lawrence in 2021: Commercial fishery and research survey data. Fisheries and Oceans Canada Canadian Science Advisory Secretariat, Research Document. 2022/027. pp. xiv + 195.

Brett, J. R. (1979). Environmental factors and growth. In W. S. Hoar, D. J. Randall, & J. R. Brett (Eds.), *Fish physiology. Volume 8. Bioenergetics and growth* (pp. 599–675). Academic Press.

Brown-Vuillemin, S., Chabot, D., Nozères, C., Tremblay, R., Sirois, P., & Robert, D. (2022). Diet composition of redfish (*Sebastes* sp.) during periods of population collapse and massive resurgence in the Gulf of St. Lawrence. *Frontiers in Marine Science*, *9*, e963039. https://doi.org/10.3389/fmars.2022.963039

Brown-Vuillemin, S., Tremblay, R., Chabot, D., Sirois, P., & Robert, D. (2023). Feeding ecology of redfish (*Sebastes* sp.) inferred from the integrated use of fatty acid profiles as complementary dietary tracers to stomach content analysis. *Journal of Fish Biology*, *102*(5), 1049–1066. https://doi.org/10.1111/jfb.15348

Brûlé, C., Benhalima, K., Roux, M. J., Parent, G. J., Chavarria, C., & Senay, C. (2024). Reduction in size-at-maturity in unprecedentedly strong cohorts of redfish (*Sebastes mentella* and *S. fasciatus*) in the Gulf of St. Lawrence and Laurentian Channel. *Journal of Fish Biology*, *104*, 1366–1385. https://doi.org/10.1111/jfb.15677

Brunel, T., & Dickey-Collas, M. (2010). Effects of temperature and population density on von Bertalanffy growth parameters in Atlantic herring: A macro-ecological analysis. *Marine Ecology Progress Series*, *405*, 15–28. https://doi.org/10.3354/meps08491

Burnham, K. P., & Anderson, D. R. (2004). Multimodel inference: Understanding AIC and BIC in model selection. *Sociological Methods & Research*, *33*(2), 261–304. https://doi.org/10.1177/0049124104268644

Burns, C., Robert, D., Sirois, P., & Plourde, S. (2022). *Régime alimentaire, croissance, et facteurs de recrutement des larves de sébaste (Sebastes mentella) dans le golfe du saint-laurent (Thèse de doctorat)*. Université du Québec à Rimouski.

Burns, C. M., Pepin, P., Plourde, S., Veillet, G., Sirois, P., & Robert, D. (2021). Revealing the relationship between feeding and growth of larval redfish (*Sebastes* sp.) in the Gulf of St. Lawrence. *ICES Journal of Marine Science*, *78*(10), 3757–3766. https://doi.org/10.1093/icesjms/fsab221

Caddy, J. F., & Gulland, J. A. (1983). Historical patterns of fish stocks. *Marine Policy*, *7*(4), 267–278.

Campana, S. E. (2001). Accuracy, precision and quality control in age determination, including a review of the use and abuse of age validation methods. *Journal of Fish Biology*, *59*(2), 197–242. https://doi.org/10.1111/j.1095-8649.2001.tb00127.x

Campana, S. E., Stefánsdóttir, R. B., Jakobsdóttir, K., & Sólmundsson, J. (2020). Shifting fish distributions in warming sub-Arctic oceans. *Scientific Reports*, *10*(1), 16448. https://doi.org/10.1038/s41598-020-73444-y

Campana, S. E., Valentin, A. E., MacLellan, S. E., & Groot, J. B. (2016). Image-enhanced burnt otoliths, bomb radiocarbon and the growth dynamics of redfish (*Sebastes mentella* and *S. fasciatus*) off the eastern coast of Canada. *Marine and Freshwater Research*, *67*(7), 925–936. https://doi.org/10.1071/MF15002

Campana, S. E., Zwanenburg, K. C. T., & Smith, J. N. (1990). 210Pb/226Ra determination of longevity in redfish. *Canadian Journal of Fisheries and Aquatic Sciences*, *47*(1), 163–165. https://doi.org/10.1139/f90-017

Casselman, J. M. (1987). Determination of age and growth. In A. H. Weatherley & H. S. Gill (Eds.), *The biology of fish growth* (pp. 209–242). Academic Press.

Denechaud, C., Smoliński, S., Geffen, A. J., Godiksen, J. A., & Campana, S. E. (2020). A century of fish growth in relation to climate change, population dynamics and exploitation. *Global Change Biology*, *26*(10), 5661–5678. https://doi.org/10.1111/gcb.15298

Devine, J. A., & Haedrich, R. L. (2011). The role of environmental conditions and exploitation in determining dynamics of redfish (*Sebastes* species) in the Northwest Atlantic. *Fisheries Oceanography*, *20*(1), 66–81. https://doi.org/10.1111/j.1365-2419.2010.00566.x

DFO. (2021). Assessment of the Gulf of St. Lawrence (4RST) Greenland halibut stock in 2020. DFO Canadian Science Advisory Secretariat, Science Advisory Report 2021/017.

DFO. (2022). Redfish (*Sebastes mentella* and *Sebastes fasciatus*) Stocks Assessment in Units 1 and 2 in 2021. DFO Canadian Science Advisory Secretariat, Science Advisory Report 2022/039.

Durant, J. M., Molinero, J. C., Ottersen, G., Reygondeau, G., Stige, L. C., & Langangen, Ø. (2019). Contrasting effects of rising temperatures on trophic interactions in marine ecosystems. *Scientific Reports*, *9*(1), 15213. https://doi.org/10.1038/s41598-019-51607-w

Dutil, J. D., Castonguay, M., Gilbert, D., & Gascon, D. (1999). Growth, condition, and environmental relationships in Atlantic cod (*Gadus morhua*) in the northern Gulf of St. Lawrence and implications for management strategies in the Northwest Atlantic. *Canadian Journal of Fisheries and Aquatic Sciences*, *56*(10), 1818–1831. https://doi.org/10.1139/f99-140

Edwards, M., & Richardson, A. (2004). Impact of climate change on marine pelagic phenology and trophic mismatch. *Nature*, *430*, 881–884. https://doi.org/10.1038/nature02808

Fox-Kemper, B., Hewitt, H. T., Xiao, C., Aðalgeirsdóttir, G., Drijfhout, S. S., Edwards, T. L., Golledge, N. R., Hemer, M., Kopp, R. E., Krinner, G., Mix, A., Notz, D., Nowicki, S., Nurhati, I. S., Ruiz, L., Sallée, J.-B., Slangen, A. B. A., & Yu, Y. (2021). Ocean, cryosphere and sea level change. In V. Masson-Delmotte, P. Zhai, A. Pirani, S. L. Connors, C. Péan, S. Berger, N. Caud, Y. Chen, L. Goldfarb, M. I. Gomis, M. Huang, K. Leitzell, E. Lonnoy, J. B. R. Matthews, T. K. Maycock, T. Waterfield, O. Yelekçi, R. Yu, & B. Zhou (Eds.), *Climate change 2021: The physical science basis. Contribution of working group I to the sixth assessment report of the intergovernmental panel on climate change* (pp. 1211–1362). Cambridge University Press.

Francis, R. I. C. C. (1990). Back-calculation of fish length: A critical review. *Journal of Fish Biology*, *36*(6), 883–902. https://doi.org/10.1111/j.1095-8649.1990.tb05636.x

Fry, F. E. J. (1971). The effect of environmental factors on the physiology of fish. In *Fish physiology* (Vol. 6, pp. 1–98). Academic press. https://doi.org/10.1016/S1546-5098(08)60146-6

Galbraith, P. S., Chassé, J., Shaw, J.-L., Dumas, J., Caverhill, C., Lefaivre, D., & Lafleur, C. (2021). Physical oceanographic conditions in the Gulf of St. Lawrence during 2020. DFO Canadian Science Advisory Secretariat, Research Document 2021/045. pp. iv + 81.

Gallucci, V. F., & Quinn, T. (1979). Reparameterizing, fitting, and testing a simple growth model. *Transactions of the American Fisheries Society*, *108*, 14–25. https://doi.org/10.1577/1548-8659(1979)108<14:RFATAS>2.0.CO;2

Gascon, D. (2003). Redfish multidisciplinary research zonal program (1995-1998): Final report. Canadian Technical Report. Fisheries and Aquatic Sciences 2462. pp. xiii + 139.

Gilbert, D., & Pettigrew, B. (1997). Interannual variability (1948–1994) of the CIL core temperature in the Gulf of St. Lawrence. *Canadian Journal of Fisheries and Aquatic Sciences*, *54*(S1), 57–67. https://doi.org/10.1139/f96-160

IPCC. (2019). Summary for policymakers. In H.-O. Pörtner, D. C. Roberts, V. Masson-Delmotte, P. Zhai, M. Tignor, E. Poloczanska, K. Mintenbeck, A. Alegría, M. Nicolai, A. Okem, J. Petzold, B. Rama, & N. M. Weyer (Eds.), *IPCC special report on the ocean and cryosphere in a changing climate* (pp. 3–35). Cambridge University Press. https://doi.org/10.1017/9781009157964.001

Jobling, M. (1996). Temperature and growth: Modulation of growth rate via temperature change. In C. M. Wood & D. G. McDonald (Eds.), *Global warming: Implications for freshwater and marine fish*. Society for Experimental Biology Seminar Series (pp. 225–253). Cambridge University Press.

Le Corre, N., Pepin, P., Han, G., & Ma, Z. (2021). Potential impact of climate change on northern shrimp habitats and connectivity on the Newfoundland and Labrador continental shelves. *Fisheries Oceanography*, *30*(3), 331–347. https://doi.org/10.1111/fog.12524

Licandeo, R., Duplisea, D. E., Senay, C., Marentette, J. R., & McAllister, M. K. (2020). Management strategies for spasmodic stocks: A Canadian Atlantic redfish fishery case study. *Canadian Journal of Fisheries and Aquatic Sciences*, *77*(4), 684–702. https://doi.org/10.1139/cjfas-2019-0210

Little, A. G., Loughland, I., & Seebacher, F. (2020). What do warming waters mean for fish physiology and fisheries? *Journal of Fish Biology*, *97*, 328–340. https://doi.org/10.1111/jfb.14402

Lorenzen, K. (2008). Fish population regulation beyond "stock and recruitment": The role of density-dependent growth in the recruited stock. *Bulletin of Marine Science*, *83*(1), 181–196.

Lorenzen, K., & Enberg, K. (2002). Density-dependent growth as a key mechanism in the regulation of fish populations: Evidence from among-population comparisons. *Proceedings of the Royal Society of London. Series B: Biological Sciences*, *269*, 49–54. https://doi.org/10.1098/rspb.2001.1853

Martínez-Silva, M. A., Vagner, M., Senay, C., & Audet, C. (2022). Using gene expression to identify the most suitable environmental conditions for growth and metabolism of juvenile deepwater redfish (*Sebastes mentella*) in the estuary and the Gulf of St. Lawrence. *ICES Journal of Marine Science*, *79*(2), 382–393. https://doi.org/10.1093/icesjms/fsab269

Martino, J. C., Fowler, A. J., Doubleday, Z. A., Grammer, G. L., & Gillanders, B. M. (2019). Using otolith chronologies to understand long-term trends and extrinsic drivers of growth in fisheries. *Ecosphere*, *10*(1), e02553. https://doi.org/10.1002/ecs2.2553

Mazerolle, M. J. (2020). AICcmodavg: Model selection and multimodel inference based on (Q)AIC(c). R package version 2.3–1. https://cran.r-project.org/package=AICcmodavg

Metcalfe, N. B., & Monaghan, P. (2001). Compensation for a bad start: Grow now, pay later? *Trends in Ecology & Evolution*, *16*(5), 254–260. https://doi.org/10.1016/S0169-5347(01)02124-3

Morrongiello, J. R., & Thresher, R. E. (2015). A statistical framework to explore ontogenetic growth variation among individuals and populations: A marine fish example. *Ecological Monographs*, *85*(1), 93–115. https://doi.org/10.1890/13-2355.1

Nedreaas, K. (1990). Age determination of northeast Atlantic *Sebastes* species. *ICES Journal of Marine Science*, *47*(2), 208–230. https://doi.org/10.1093/icesjms/47.2.208

Norse, E. A., Brooke, S., Cheung, W. W. L., Clark, M. R., Ekeland, I., Froese, R., Gjerde, K. M., Haedrich, R. L., Heppell, S. S., Morato, T., Morgan, L. E., Pauly, D., Sumaila, R., & Watson, R. (2012). Sustainability of deep-sea fisheries. *Marine Policy*, *36*(2), 307–320. https://doi.org/10.1016/j.marpol.2011.06.008

O'Connor, C. M., Norris, D. R., Crossin, G. T., & Cooke, S. J. (2014). Biological carryover effects: Linking common concepts and mechanisms in ecology and evolution. *Ecosphere*, *5*(3), 1–11. https://doi.org/10.1890/ES13-00388.1

Ogle, D. H. (2013a). fishR Vignette – Back-calculation of fish length. http://derekogle.com/fishR/examples/oldFishRVignettes/Backcalculation.pdf

Ogle, D. H. (2013b). FishR Vignette – Von Bertalanffy growth models. http://derekogle.com/fishR/examples/oldFishRVignettes/VonBertalanffy.pdf

Ogle, D. H., Doll, J. C., Wheeler, A. P., & Dinno, A. (2023). FSA: Simple fisheries stock assessment methods. R Package Version 0.9.5. https://fishr-core-team.github.io/FSA/

Parmesan, C., & Yohe, G. (2003). A globally coherent fingerprint of climate change impacts across natural systems. *Nature*, *421*(6918), 37–42. https://doi.org/10.1038/nature01286

Pepin, P. (2015). Reconsidering the impossible—Linking environmental drivers to growth, mortality, and recruitment of fish. *Canadian Journal of Fisheries and Aquatic Sciences*, *73*(2), 205–215. https://doi.org/10.1139/cjfas-2015-0091

Pereira, L. S., Agostinho, A. A., & Winemiller, K. O. (2017). Revisiting cannibalism in fishes. *Reviews in Fish Biology and Fisheries*, *27*, 499–513. https://doi.org/10.1007/s11160-017-9469-y

Perry, A. L., Low, P. J., Ellis, J. R., & Reynolds, J. D. (2005). Ecology: Climate change and distribution shifts in marine fishes. *Science*, *308*, 1912–1915. https://doi.org/10.1126/science.1111322

Pillet, M., Dupont-Prinet, A., Chabot, D., Tremblay, R., & Audet, C. (2016). Effects of exposure to hypoxia on metabolic pathways in northern shrimp (*Pandalus borealis*) and Greenland halibut (*Reinhardtius hippoglossoides*). *Journal of Experimental Marine Biology and Ecology*, *483*, 88–96. https://doi.org/10.1016/j.jembe.2016.07.002

Poloczanska, E. S., Brown, C. J., Sydeman, W. J., Kiessling, W., Schoeman, D. S., Moore, P. J., Brander, K., Bruno, J. F., Buckley, L. B., Burrows, M. T., Duarte, C., Halpern, B. S., Holding, J., Kappel, C. V., O'Connor, M. I., Pandolfi, J. M., Parmesan, C., Schwing, F., Thompson, S. A., & Richardson, A. J. (2013). Global imprint of climate change on marine life. *Nature Climate Change*, *3*(10), 919–925. https://doi.org/10.1038/nclimate1958

R Core Team. (2020). *R: A language and environment for statistical computing*. R Foundation for Statistical Computing. http://www.r-project.org

Ricker, W. E. (1954). Stock and recruitment. *Journal of the Fisheries Research Board of Canada*, *11*(5), 559–623. https://doi.org/10.1139/f54-039

Rose, K. A., Cowan, J. H., Jr., Winemiller, K. O., Myers, R. A., & Hilborn, R. (2001). Compensatory density dependence in fish populations: Importance, controversy, understanding and prognosis. *Fish and Fisheries*, *2*(4), 293–327. https://doi.org/10.1046/j.1467-2960.2001.00056.x

Saborido-Rey, F., Garabana, D., & Cervino, S. (2004). Age and growth of redfish (*Sebastes marinus*, *S. mentella*, and *S. fasciatus*) on the Flemish cap (Northwest Atlantic). *ICES Journal of Marine Science*, *61*(2), 231–242. https://doi.org/10.1016/j.icesjms.2003.11.003

Schneider, C. A., Rasband, W. S., & Eliceiri, K. W. (2012). NIH image to ImageJ: 25 years of image analysis. *Nature Methods*, *9*(7), 671–675. https://doi.org/10.1038/nmeth.2089

Senay, C., Bermingham, T., Parent, G. J., Benoît, H. P., Parent, E., & Bourret, A. (2022). Identifying two redfish species, *Sebastes mentella* and *S. fasciatus*, in fishery and survey catches using anal fin ray count in units 1 and 2. DFO Canadian technical report. *Fisheries Aquatic Science*, *3445*, viii + 46.

Senay, C., Ouellette-Plante, J., Bourdages, H., Bermingham, T., Gauthier, J., Parent, G., Chabot, D., & Duplisea, D. (2021). Unit 1 Redfish (*Sebastes mentella* and *S. fasciatus*) stock status in 2019 and updated information on population structure, biology, ecology, and current fishery closures. DFO Canadian Science Advisory Secretariat. Research Document 2021/015. pp. xi + 119.

Shelton, A. O., & Mangel, M. (2011). Fluctuations of fish populations and the magnifying effects of fishing. *Proceedings of the National Academy of Sciences of the United States of America*, *108*(17), 7075–7080. https://doi.org/10.1073/pnas.1100334108

Sinclair, A. F., Swain, D. P., & Hanson, J. M. (2002). Disentangling the effects of size-selective mortality, density, and temperature on length-at-age. *Canadian Journal of Fisheries and Aquatic Sciences*, *59*(2), 372–382. https://doi.org/10.1139/f02-014

Smith, C., & Reay, P. (1991). Cannibalism in teleost fish. *Reviews in Fish Biology and Fisheries*, *1*, 41–64. https://doi.org/10.1007/BF00042661

Smoliński, S., Deplanque-Lasserre, J., Hjörleifsson, E., Geffen, A. J., Godiksen, J. A., & Campana, S. E. (2020). Century-long cod otolith biochronology reveals individual growth plasticity in response to temperature. *Scientific Reports*, *10*(1), 1–13. https://doi.org/10.1038/s41598-020-73652-6

Starr, M., Harvey, M., Galbraith, P. S., Gilbert, D., Chabot, D., & Therriault, J. C. (2002). Recent intrusion of Labrador shelf waters into the Gulf of St. Lawrence and its influence on the plankton community and higher trophic levels. In *2002 ICES annual science conference and ICES centenary*. ICES.

Stransky, C., Gudmundsdóttir, S., Sigurdsson, T., Lemvig, S., Nedreaas, K., & Saborido-Rey, F. (2005). Age determination and growth of Atlantic redfish (*Sebastes marinus* and *S. mentella*): Bias and precision of age readers and otolith preparation methods. *ICES Journal of Marine Science*, *62*(4), 655–670.

Swain, D. P., Sinclair, A. F., Castonguay, M., Chouinard, G. A., Drinkwater, K. F., Fanning, L. P., & Clark, D. S. (2003).

Density-versus temperature-dependent growth of Atlantic cod (*Gadus morhua*) in the Gulf of St. Lawrence and on the Scotian shelf. *Fisheries Research*, *59*(3), 327–341. https://doi.org/10.1016/S0165-7836(02)00027-9

Tanaka, S., Togoshi, S., Yasue, N., Burns, C. M., Robert, D., & Takasuka, A. (2023). Revisiting the role of early life growth for survival potential in three clupeoid species. *Fisheries Oceanography*, *32*(2), 245–254. https://doi.org/10.1111/fog.12626

Trippel, E. A. (1995). Age at maturity as a stress indicator in fisheries. *Bioscience*, *45*(11), 759–771. https://doi.org/10.2307/1312628

van der Sleen, P., Stransky, C., Morrongiello, J. R., Haslob, H., Peharda, M., & Black, B. A. (2018). Otolith increments in European plaice (*Pleuronectes platessa*) reveal temperature and density-dependent effects on growth. *ICES Journal of Marine Science*, *75*(5), 1655–1663. https://doi.org/10.1093/icesjms/fsy032

Vigliola, L., & Meekan, M. G. (2009). The back-calculation of fish growth from otoliths. In B. S. Green, G. A. Begg, G. Carlos, & B. M. Mapstone (Eds.), *Tropical fish otoliths: Information for assessment, management and ecology* (pp. 174–211). Springer.

Weisberg, S., Spangler, G., & Richmond, L. S. (2010). Mixed effects models for fish growth. *Canadian Journal of Fisheries and Aquatic Sciences*, *67*(2), 269–277. https://doi.org/10.1139/F09-18

Whitten, A. R., Klaer, N. L., Tuck, G. N., & Day, R. W. (2013). Accounting for cohort-specific variable growth in fisheries stock assessments: A case study from south-eastern Australia. *Fisheries Research*, *142*, 27–36. https://doi.org/10.1016/j.fishres.2012.06.021

Zimmermann, F., Ricard, D., & Heino, M. (2018). Density regulation in Northeast Atlantic fish populations: Density dependence is stronger in recruitment than in somatic growth. *Journal of Animal Ecology*, *87*(3), 672–681.

Zuur, A., Ieno, E. N., Walker, N., Saveliev, A. A., & Smith, G. M. (2009). *Mixed effects models and extensions in ecology with R*. Springer Science & Business Media.

SUPPORTING INFORMATION

Additional supporting information can be found online in the Supporting Information section at the end of this article.

How to cite this article: Coussau, L., Morissette, O., Robert, D., & Sirois, P. (2024). Drivers of growth in strong year classes of the deepwater redfish (*Sebastes mentella*) population from the Gulf of St. Lawrence derived from otolith increment-based growth chronologies. *Journal of Fish Biology*, 1–15. https://doi.org/10.1111/jfb.15903